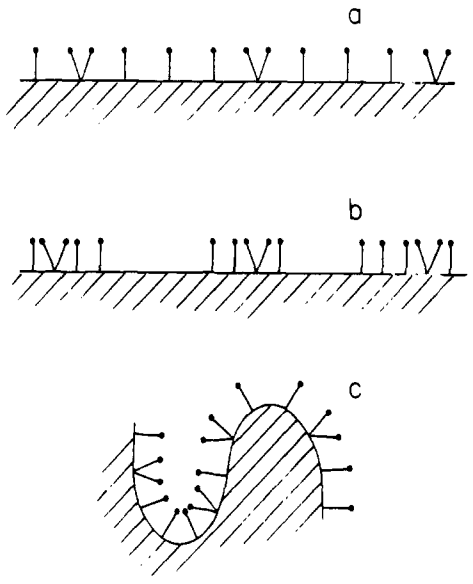


**Figure 5.** (a) The homogeneous view of adsorption sites of silica.[23] (b) The heterogeneous view of adsorption sites.[25] See, also Figure 2 in ref 24. (c) The suggestion of this study: a homogeneous distribution of silanols form clusters due to surface concave and convex features.

Unger and Lochmüller's pictures coincide, as is clearly evident in Figure 5: both homogeneous distribution *and* clustering describe the situation of silanols on the surface; concave zones have a high density of adsorption sites and convex zones, a smaller density. In other words, the very existence of surface irregularities and of a specific pore size distribution, and in particular the left tail of this distribution, are sufficient to account for heterogeneity of adsorption sites. I am tempted to claim that the *sole* origin of surface heterogeneity in silica is geometric in nature. This geometric picture of heterogeneity is also in keeping with known observations[43] that activity is a function of coverage. One expects that at very low $\theta$ values the first adsorption sites to be occupied would be the very narrow pores and the highly concave surface features, which (Figure 5c) are the densest in adsorption sites; then, as $\theta$ grows, the adsorbate–adsorbent interactive system moves up the left tail of the pore distribution curve to zones which are less crowded, and surface reactions are accordingly affected. In particular I mention the environmental relaxation around an excited state. Unlike solution, in which most relaxation and resolvation movements are those of the small solvent molecules around a large solute molecule,[44] on a surface, this relaxation must be a combination of the adsorbate molecular motions together with rotations of surface groups (e.g., around an Si–OH bond). For silica-60 Å with $D \rightarrow 3.0$, on which the dual fluorescence of 1-(*N*,*N*-dimethylamino)-4-benzonitrile was studied,[36] we found that this process is extremely, almost solventlike ($D = 3.0$), efficient and is less efficient for silica-1000 Å, with $D = 2.15$.[40]

## 5. Summary

Environmental geometry is a primary factor in photochemical surface reactions. This parameter, which is unique to surface processes, has been overlooked in many recent surface photochemistry studies. In this report, I showed that ignoring geometrical considerations may lead to inaccuracies in the evaluation and interpretation of experimental observations. I suggested ways for correct processing of experimental data obtained from irregular surfaces. These include both classical surface science tools and the use of empirical surface science scaling laws which have been interpreted as reflecting fractal properties of the heterogeneous environment. I have shown how surface geometry affects properties such as intermolecular distances, surface concentrations, available surface for reaction and for excited intermediates, and surface heterogeneity.

**Acknowledgment.** I thank M. Ottolenghi, J. Samuel, and D. Farin for useful discussions, P. de-Mayo, N. J. Turro, and N. B. Zimmt for helpful correspondence, and M. L. Kagan for assistance in making the computations of Figures 1–4. Supported by the U.S.–Israel Binational Science Foundation and by the Israel National Academy of Sciences.

(43) e.g., Al-Ekabi, H.; de Mayo, P. *J. Phys. Chem.* **1985**, *89*, 5815.

(44) Wang, Y.; Eisenthal, K. B. *J. Chem. Phys.* **1982**, *77*, 6076.

# Mononuclear Oxo- and Sulfidomolybdenum(IV) Complexes: Syntheses and Crystal Structures of $\{HB(Me_2C_3N_2H)_3\}MoE(S_2CNEt_2)$ (E = O, S) and Related Complexes

**Charles G. Young, Sue A. Roberts, Richard B. Ortega, and John H. Enemark***

*Contribution from the Department of Chemistry, University of Arizona, Tucson, Arizona 85721.*
*Received August 27, 1986*

**Abstract:** The syntheses, structures, and properties of mononuclear oxo- and sulfidomolybdenum(IV) complexes with hydrotris(3,5-dimethyl-1-pyrazolyl)borate, $HB(Me_2pz)_3^-$, and dithiocarbamate ligands are described. The reactions of $MoO(S_2CNR_2)_2$ (R = Me, Et, *n*-Pr, *n*-Bu) with $K\{HB(Me_2pz)_3\}$ in refluxing toluene yield the green, diamagnetic, air-stable complexes $\{HB(Me_2pz)_3\}MoO(S_2CNR_2)$. The complex $\{HB(Me_2pz)_3\}MoO(S_2CNEt_2)$ crystallizes in the monoclinic space group $P2_1/c$ with $a = 8.303$ (2) Å, $b = 21.710$ (4) Å, $c = 14.475$ (3) Å, $\beta = 100.75$ (2)°, $Z = 4$. The molybdenum atom is in a distorted octahedral coordination environment composed of *fac*-tridentate $HB(Me_2pz)_3^-$, terminal oxo (Mo=O = 1.669 (3) Å), and bidentate $S_2CNEt_2^-$ ligands. The reaction of these oxo complexes with boron sulfide in dichloromethane yields the gold-yellow, diamagnetic sulfido analogues $\{HB(Me_2pz)_3\}MoS(S_2CNR_2)$. The compound $\{HB(Me_2pz)_3\}MoS(S_2CNEt_2)\cdot CH_2Cl_2$ crystallizes in the orthorhombic space group $P2_12_12_1$ with $a = 7.967$ (3) Å, $b = 14.314$ (5) Å, $c = 26.15$ (1) Å, $Z = 4$. The coordination geometry is similar to that of the oxo analogue, with Mo=S = 2.129 (2) Å.

"Oxo-type" molybdoenzymes such as sulfite oxidase, xanthine oxidase, and xanthine dehydrogenase are of considerable current interest.[1,2] Their molybdenum centers have been probed directly by X-ray absorption spectroscopy, especially extended X-ray

0002-7863/87/1509-2938$01.50/0 

absorption fine structure (EXAFS),[3] and by electron paramagnetic resonance (EPR) spectroscopy.[4] The oxidized form of sulfite oxidase is postulated to contain *cis*-dioxomolybdenum(VI) (see ref 57) centers (A), whereas the oxidized active forms of xanthine


A B C D

oxidase and xanthine dehydrogenase are postulated to contain oxosulfidomolybdenum(VI) centers (B). The enzymes exhibit transient Mo(V) states under a variety of conditions, and, on the basis of rapid freeze EPR experiments, both monooxo- and monosulfidomolybdenum(V) ($C^{3+}$, $D^{3+}$) centers have been proposed for these states.[4] EXAFS studies on the reduced Mo(IV) states of the enzymes are consistent with the presence of monooxomolybdenum(IV) centers ($C^{2+}$). There is also good evidence that the molybdenum centers are bound to a common molybdenum cofactor which is postulated to contain a bidentate sulfur–donor chelate ligand incorporating pterin and phosphate functionalities[5,6] (E).

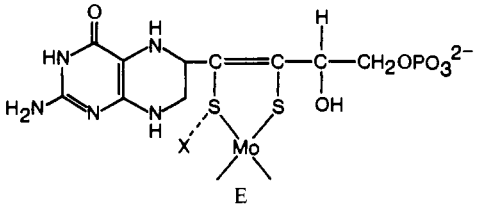


E

No oxo-type molybdoenzyme has yet been characterized by an X-ray crystal structure determination. Consequently, the present descriptions of the coordination environments of the molybdenum centers in these enzymes rest upon the spectroscopic and chemical properties of well-characterized molybdenum complexes. The challenge to synthetic chemists is to prepare mononuclear complexes which contain fragments A through D and which also incorporate some of the structural features of E, such as cis sulfur–donor atoms.

Numerous complexes containing the *cis*-dioxomolybdenum(VI) unit (A) and one or more sulfur–donor ligands have been reported,[7a] and some of these catalyze the oxidation of tertiary phosphines by sulfoxides.[7] In contrast, complexes containing the oxosulfidomolybdenum(VI) unit (B) are rare; representative examples include the thiomolybdates[8] and the skew trapezoidal bipyramidal complexes, *cis*-$MoOS(ONR_2)_2$.[9,10] Oxo- and sulfidomolybdenum(V) units ($C^{3+}$, $D^{3+}$) show a marked propensity toward the formation of binuclear species, but mononuclear oxomolybdenum(V) complexes have been prepared under rigorously anhydrous conditions or by the use of sterically protective ligands.[11,12] There is one example of a mononuclear sulfidomolybdenum(V) complex.[12b] Mononuclear oxomolybdenum(IV) complexes ($C^{2+}$) are well known, but most sulfidomolybdenum(IV) centers ($D^{2+}$) occur in bi-, tri-, and tetranuclear complexes.[13] Only two mononuclear sulfidomolybdenum(IV) complexes, $[MoS(S_4)_2]^{2-}$ and $[MoS(CS_4)_2]^{2-}$, have been reported.[14,15]

Recently, we have prepared an extensive series of stable, mononuclear oxomolybdenum(V) complexes of hydrotris(3,5-dimethyl-1-pyrazolyl)borate, $HB(Me_2pz)_3^-$.[12a] This ligand forms a protective steric pocket about the molybdenum atom, thereby limiting the formation of binuclear species and restricting the complexes to *facial* six-coordinate geometries. The unusual stability of the $\{HB(Me_2pz)_3\}MoOXY$ (X, Y = monoanions) complexes and their facile electrochemical reduction to oxomolybdenum(IV) complexes prompted us to exploit the $HB(Me_2pz)_3^-$ ligand in the development of new oxo- and sulfidomolybdenum(IV) chemistry. We report here the synthesis and characterization of the six-coordinate oxo- and sulfidomolybdenum(IV) complexes, $\{HB(Me_2pz)_3\}MoE(S_2CNR_2)$ (E = O, S; R = Me, Et, *n*-Pr, *n*-Bu), and the X-ray crystal structures of the analogous pair, $\{HB(Me_2pz)_3\}MoE(S_2CNEt_2)$.

## Experimental Section

**Syntheses.** All reactions were performed under an atmosphere of pure dinitrogen by using standard inert-atmosphere techniques. The solvents employed throughout were dried, distilled, and deoxygenated before use. The materials $K\{HB(Me_2pz)_3\}$[16] and *cis*-$MoO_2(S_2CNR_2)_2$[17] (R = Me, Et, *n*-Pr, *n*-Bu) were prepared according to literature procedures. Boron sulfide (Morton Thiokol Inc., Alfa Products) was used as received.

**$\{HB(Me_2pz)_3\}MoO(S_2CNR_2)$ Complexes.** A suspension of the appropriate *cis*-$MoO_2(S_2CNR_2)_2$ complex (5 mmol) and triphenylphosphine (1.31 g, 5 mmol) in toluene (50 mL, 80 mL for **1a**) was refluxed for 1–2 h and then allowed to cool. Following the addition of $K\{HB(Me_2pz)_3\}$ (1.71 g, 5.1 mmol), the suspension was refluxed for a further 18 h. The green crystalline product was isolated by filtration in air, washed with toluene/methanol (1:1) and methanol, and vacuum dried. The complexes were recrystallized from dichloromethane by the addition of methanol. The *n*-Bu derivative did not precipitate from the reaction mixture. Instead, the reaction mixture was evaporated to dryness (in vacuo), and the residue was chromatographed on silica gel (Kieselgel 60, Fluka) by using dichloromethane as solvent. The green product was recrystallized from dichloromethane/methanol to yield the solvate **1d**·$CH_2Cl_2$.

**1a**: R = Me, yield 1.3 g (50%). Anal. Calcd for $C_{18}H_{28}BMoN_7OS_2$: C, 40.84; H, 5.33; N, 18.52; S, 12.11. Found: C, 40.7; H, 5.3; N, 18.5; S, 12.1%.

**1b**: R = Et, yield 2.1 g (76%). Anal. Calcd for $C_{20}H_{32}BMoN_7OS_2$: C, 43.10; H, 5.79; N, 17.59; S, 11.50. Found: C, 42.9; H, 5.7; N, 17.5; S, 11.4.

**1c**: R = *n*-Pr, yield 2.2 g (75%). Anal. Calcd for $C_{22}H_{36}BMoN_7OS_2$: C, 45.13; H, 6.20; N, 16.80; S, 10.95. Found: C, 45.0; H, 6.3; N, 17.1; S, 11.1.

**1d**·$CH_2Cl_2$: R = *n*-Bu, yield 1.9 g (55%). Anal. Calcd for $C_{25}H_{42}BCl_2MoN_7OS_2$: C, 42.99; H, 6.06; N, 14.03; S, 9.18. Found: C, 43.3; H, 6.2; N, 14.4; S, 9.4.

**$\{HB(Me_2pz)_3\}MoS(S_2CNR_2)$ Complexes.** A solution of the appropriate $\{HB(Me_2pz)_3\}MoO(S_2CNR_2)$ complex (1.8 mmol) in dichloromethane (40 mL) was treated with boron sulfide (0.6 g, 5.2 mmol) and stirred for 24 h. The mixture was filtered, and the brown filtrate was evaporated to dryness in vacuo. The residue was dissolved in dichloromethane (~10 mL) and treated with methanol (effervescence) to precipitate yellow crystals of the product. The complexes were recrystallized

(1) Spence, J. T. *Coord. Chem. Rev.* **1983**, *48*, 59–82.
(2) *Molybdenum and Molybdenum-Containing Enzymes*; Coughlan, M. P., Ed.; Pergamon: New York, 1980.
(3) Cramer, S. P. In *Advances in Inorganic and Bioinorganic Mechanisms*; Sykes, A. G., Ed.; Academic: New York, 1983; Vol. 2, pp 259–316.
(4) Bray, R. C. *Adv. Enzymol. Relat. Areas Mol. Biol.* **1980**, *51*, 107–165.
(5) Johnson, J. L.; Rajagopolan, K. V. *Proc. Natl. Acad. Sci. U.S.A.* **1982**, *79*, 6856–6860.
(6) Stiefel, E. I.; Carmer, S. P. In *Molybdenum Enzymes*; Spiro, T. G., Ed.; Wiley-Interscience: New York, 1985; pp 89–116.
(7) (a) Berg, J. M.; Holm, R. H. *J. Am. Chem. Soc.* **1985**, *107*, 925–932, and references therein. (b) Kaul, B. B.; Enemark, J. H.; Merbs, S. L.; Spence, J. T. *J. Am. Chem. Soc.* **1985**, *107*, 2885.
(8) Diemann, E.; Muller, A. *Coord. Chem. Rev.* **1973**, *10*, 79–122.
(9) (a) Hofer, E.; Holzbach, W.; Wieghardt, K. *Angew. Chem., Int. Ed. Engl.* **1981**, *20*, 282–283. (b) Wieghardt, K.; Hahn, M.; Weiss, J.; Swiridoff, W. *Z. Anorg. Allg. Chem.* **1982**, *492*, 164–174.
(10) Bristow, S.; Collison, D.; Garner, C. D.; Clegg, W. *J. Chem. Soc., Dalton Trans.* **1983**, 2495–2499.
(11) Taylor, R. D.; Todd, P. G.; Chasteen, N. D.; Spence, J. T. *Inorg. Chem.* **1979**, *18*, 44–48.
(12) (a) Cleland, W. E., Jr.; Barnhart, K. M.; Yamanouchi, K.; Collison, D.; Mabbs, F. E.; Ortega, R. B.; Enemark, J. H. *Inorg. Chem.*, in press. (b) Young, C. G.; Collison, D.; Mabbs, F. E.; Enemark, J. H., to be submitted for publication.
(13) Selected references include the following: (a) Brunner, H.; Meier, W.; Wachter, J.; Goggolz, E.; Zahn, T.; Ziegler, M. L. *Organometallics* **1982**, *1*, 1107–1113. (b) Muller, A.; Pohl, S.; Dartmann, M.; Cohen, J. P.; Bennett, J. M.; Kirchner, R. M. *Z. Naturforsch., B: Anorg. Chem., Org. Chem.* **1979**, *34B*, 434–436. (c) Howlader, N. C.; Haight, G. P., Jr.; Hambley, T. W.; Lawrance, G. A.; Rahmoeller, K. M.; Snow, M. R. *Aust. J. Chem.* **1983**, *36*, 377–383. (d) Kathirgamanathane, P.; Martinez, M.; Sykes, A. G. *J. Chem. Soc., Chem. Commun.* **1985**, 953–954. (e) Kathirgamanathane, P.; Martinez, M.; Sykes, A. G. *Ibid.* **1985**, 1437–1438.
(14) (a) Simhon, E. D.; Baenziger, N. C.; Kanatzidis, M.; Draganjac, M.; Coucouvanis, D. *J. Am. Chem. Soc.* **1981**, *103*, 1218–1219. (b) Draganjac, M.; Simhon, E.; Chan, L. T.; Kanatzidis, M.; Baenziger, N. C.; Coucouvanis, D. *Inorg. Chem.* **1982**, *21*, 3321–3322.
(15) (a) Coucouvanis, D.; Draganjac, M. *J. Am. Chem. Soc.* **1982**, *104*, 6820–6822. (b) Coucouvanis, D.; Hadjikyriacou, A.; Draganjac, M.; Kanatzidis, M. G.; Ileperuma, O. *Polyhedron* **1986**, *5*, 349–356.
(16) Trofimenko, S. *J. Am. Chem. Soc.* **1967**, *89*, 6288–6294.
(17) Moore, F. W.; Larson, M. L. *Inorg. Chem.* **1967**, *6*, 998–1003.

from dichloromethane by the addition of methanol. The methyl derivative was sometimes difficult to free from $\{HB(Me_2pz)_3\}Mo_2S_4(S_2CNMe_2)$ byproduct.

**2a**: R = Me, yield 0.68 g (70%). Anal. Calcd for $C_{18}H_{28}BMoN_7S_3$: C, 39.64; H, 5.17; N, 17.98; S, 17.63. Found: C, 39.2; H, 5.2; N, 17.8; S, 17.0.

**2b**: R = Et, yield 0.88 g (85%). Anal. Calcd for $C_{20}H_{32}BMoN_7S_3$: C, 41.89; H, 5.63; N, 17.09; S, 16.77. Found: C, 41.7; H, 5.7; N, 17.1; S, 16.7.

**2c**: R = *n*-Pr, yield 0.92 g (85%). Anal. Calcd for $C_{22}H_{36}BMoN_7S_3$: C, 43.93; H, 6.03; N, 16.30; S, 15.99. Found: C, 43.7; H, 6.1; N, 16.2; S, 16.0.

**2d**: R = *n*-Bu, yield 1.0 g (88%). Anal. Calcd for $C_{24}H_{40}BMoN_7S_3$: C, 45.79; H, 6.40; N, 15.57; S, 15.28. Found: C, 45.6; H, 6.4; N, 15.5; S, 15.2.

**Crystal Structure Determinations.** Crystal data for **1b** and **2b**·$CH_2Cl_2$, together with details of the X-ray diffraction experiments, are reported in Table I. Green crystals of **1b** were grown by slow diffusion of methanol into a dichloromethane solution of the complex. The compound crystallizes in monoclinic space group $P2_1/c$ (no. 14,[18] systematic absences: $h0l$, $l = 2n + 1$; $0k0$, $k = 2n + 1$). Cell constants and an orientation matrix for data collection were obtained from least-squares refinement by using setting angles of 24 reflections in the range $12 < 2\theta < 19°$. During the data collection, the intensities of two representative reflections were measured every 48 reflections; no decay was detected. The position of the Mo atom was determined from the Patterson function. The remaining atoms were located by successive structure factor calculations and difference electron density maps. Hydrogen atoms were located and added to the structure factor calculation, but their positions were not refined. Refinement employed 2840 reflections having $I > 3\sigma(I)$ and converged with unweighted and weighted agreement factors of 0.037 and 0.042, respectively.

Gold-yellow crystals of **2b**·$CH_2Cl_2$ were grown under anaerobic conditions by slow diffusion of methanol into a dichloromethane solution of the compound. The compound crystallizes in orthorhombic space group $P2_12_12_1$ (no. 19,[18] systematic absences: $h00$, $h = 2n + 1$; $0k0$, $k = 2n + 1$; $00l$, $l = 2n + 1$). Cell constants and an orientation matrix for data collection were obtained from least-squares refinement by using setting angles of 20 reflections in the range $10 < 2\theta < 20°$. During data collection, the intensities of three representative reflections were measured every 100 reflections; no crystal decay or electronic instability was detected. The position of the Mo atom was determined from the Patterson function. The remaining atoms were located as in **1b**. Hydrogen atoms were placed in idealized positions and added to the structure factor calculation, but their positions were not refined. Refinement employed 2324 reflections having $I > 3\sigma(I)$ and converged with unweighted and weighted agreement factors of 0.035 and 0.042, respectively. The space group is acentric; however, refinement of the other enantiomer produced no change in $R_w$. Consequently, the correct enantiomer cannot be determined from this data set.

For both structures, scattering factors were taken from Cromer and Waber.[19] Anomalous dispersion effects were included in $F_c$ for all non-hydrogen atoms; the values of $\Delta f'$ and $\Delta f''$ were those of Cromer.[20] All calculations were performed on a PDP-11/34a computer by using SDP-PLUS.[21]

**Other Measurements.** Infrared spectra were recorded as KBr discs on a Perkin-Elmer 983 spectrophotometer. Electronic spectra were obtained in dichloromethane on an IBM 9420 spectrophotometer. Proton magnetic resonance spectra were obtained on a Bruker WH 400-MHz NMR spectrometer by using tetramethylsilane as internal standard. The $^{95}Mo$ NMR spectra were recorded on a Bruker WM 250-MHz NMR spectrometer by using methodology described elsewhere.[22] $^{95}Mo$ chemical shifts are referenced to an external standard of 2 M $Na_2[MoO_4]$ in $D_2O$, effective pH 11 (positive chemical shifts are deshielded relative to the reference). Cyclic voltammograms of $10^{-3}$ M solutions of the compounds were recorded either at a glassy carbon or Pt disk-working electrode in dichloromethane/0.05 M $Bu_4NBF_4$ or in dimethylformamide/0.1 M $Bu_4BF_4$ on an IBM EC/225 voltammetric analyzer. The experiments employed a saturated calomel (SCE) reference electrode and a platinum wire auxiliary electrode. Microanalyses were performed by Atlantic Microlabs Inc.

**Table I**

| | **1b** | **2b**·$CH_2Cl_2$ |
|---|---|---|
| **A. Crystal Data** | | |
| chem formula | $C_{20}H_{32}BMoN_7OS_2$ | $C_{21}H_{34}BCl_2MoN_7S_3$ |
| fw | 557.40 | 658.40 |
| cryst color | green | orange-yellow |
| cryst dimens, mm | 0.17 × 0.12 × 0.06 | 0.47 × 0.30 × 0.05 |
| peak width at half-height | 0.25 | 0.30 |
| Mo Kα radiation | λ = 0.71073 Å | |
| temp, °C | 23 ± 1 | |
| space group | $P2_1/c$ | $P2_12_12_1$ |
| *a*, Å | 8.303 (2) | 7.967 (3) |
| *b*, Å | 21.710 (4) | 14.314 (5) |
| *c*, Å | 14.475 (3) | 26.150 (10) |
| β, deg | 100.75 (2) | |
| *V*, Å$^3$ | 2563.4 | 2982.1 |
| *Z* | 4 | 4 |
| ρ calcd, g cm$^{-3}$ | 1.44 | 1.47 |
| ρ measd, g cm$^{-3}$ | 1.47 | 1.46 |
| μ, cm$^{-1}$ | 6.8 | 8.3 |
| **B. Intensity Measurements** | | |
| instrument | Syntex (Nicolet) $P2_1$, with modified software | |
| monochromator | graphite crystal, incident beam | |
| scan type | θ–2θ | |
| scan rate, deg min$^{-1}$ | 1.5–10 | 1.5–8 |
| scan width, deg | Kα$_1$ − 1.0 to Kα$_2$ + 1.1 | Kα$_1$ − 1.1 to Kα$_2$ + 1.1 |
| max 2θ, deg | 50 | 50 |
| no. of reflcns measd | 5024 | 3043 |
| corrcns | Lorentz-polarization | analyt absrptn (0.792–0.958; av 0.937) |
| **C. Solution and Refinement** | | |
| solution | Patterson method | |
| hydrogen atoms | found, not refined calcd, not refined | |
| refinement | full matrix least-squares | |
| minimization function | $\sum w(\|F_o\| - \|F_c\|)^2$ | |
| least-squares weights | $4F_o^2/\sigma^2(F_o)^2$ | |
| anamolous dispersion | all non-hydrogen atoms | |
| no. of reflcns included | 2805 | 2324 |
| no. of parameters refined | 289 | 316 |
| unweighted agreement factor | 0.037 | 0.035 |
| weighted agreement factor | 0.042 | 0.042 |
| esd of obsrvn of unit wt | 1.21 | 1.42 |
| convergence, largest shift | 0.04 | 0.26 |
| high peak in final difference map, eÅ$^{-3}$ | 0.33 | 0.40 |

[a] $R = \sum||F_o| - |F_c||/\sum|F_o|$. [b] $R_w = (\sum w(|F_o| - |F_c|)^2/\sum wF_o^2)^{1/2}$.

## Results and Discussion

**Syntheses.** The green, diamagnetic, air-stable oxo complexes **1a–1d** were readily prepared in high yield and purity by the reactions of $MoO(S_2CNR_2)_2$ complexes with $K\{HB(Me_2pz)_3\}$ in refluxing toluene (eq 1). The $MoO(S_2CNR_2)_2$ complexes were conveniently prepared in situ via the oxygen atom transfer reactions of *cis*-$MoO_2(S_2CNR_2)_2$ complexes and $PPh_3$ (eq 2).[23]

$$MoO(S_2CNR_2)_2 + K\{HB(Me_2pz)_3\} \rightarrow \{HB(Me_2pz)_3\}MoO(S_2CNR_2) + KS_2CNR_2 \quad (1)$$

$$cis\text{-}MoO_2(S_2CNR_2)_2 + PPh_3 \rightarrow MoO(S_2CNR_2)_2 + OPPh_3 \quad (2)$$

(18) *International Tables for Crystallography*; Hahn, T., Ed.; Reidel: Dordrecht, 1983; Vol. A, p 174 ($P2_1/c$), p 196 ($P2_12_12_1$).
(19) Cromer, D. T.; Waber, J. T. *International Tables for X-ray Crystallography*; Kynoch: Birmingham, 1974; Vol. IV, Table 2.2B.
(20) Cromer, D. T. In *International Tables for X-ray Crystallography*; Kynoch: Birmingham, 1974; Vol. IV, Table 2.3.1.
(21) Frenz, B. A. In *Computing in Crystallography*; Schenk, H., Olthof-Hazelkamp, R., van Konigsveld, H., Bassi, G. C., Eds.; Delft University: Delft, 1978; pp 64–71.
(22) Young, C. G.; Enemark, J. H. *Inorg. Chem.* **1985**, *24*, 4416–4419.

**Table II.** Positional and Isotropic Thermal Parameters for $\{HB(Me_2pz)_3\}MoO(S_2CNEt_2)$[a]

| atom | x | y | z | $B_{eq}$ (Å$^2$) |
|---|---|---|---|---|
| Mo | 0.01078 (5) | 0.16694 (2) | 0.40054 (3) | 2.432 (8) |
| S1 | −0.1238 (2) | 0.16335 (7) | 0.53609 (8) | 3.23 (3) |
| S2 | −0.1583 (2) | 0.25958 (6) | 0.39898 (8) | 3.27 (3) |
| O | 0.1929 (4) | 0.1957 (2) | 0.4500 (2) | 3.51 (8) |
| N11 | −0.2268 (5) | 0.1131 (2) | 0.3091 (3) | 2.85 (9) |
| N12 | −0.1893 (5) | 0.0693 (2) | 0.2469 (3) | 2.97 (9) |
| N21 | 0.0985 (5) | 0.0723 (2) | 0.4035 (3) | 3.01 (9) |
| N22 | 0.0964 (5) | 0.0394 (2) | 0.3217 (3) | 3.07 (9) |
| N31 | 0.0600 (5) | 0.1727 (2) | 0.2579 (3) | 2.70 (8) |
| N32 | 0.0487 (5) | 0.1229 (2) | 0.1994 (3) | 2.89 (9) |
| N41 | −0.2825 (6) | 0.2688 (2) | 0.5582 (3) | 3.6 (1) |
| C11 | −0.3901 (7) | 0.1095 (3) | 0.3041 (4) | 3.3 (1) |
| C12 | −0.4561 (7) | 0.0643 (3) | 0.2403 (4) | 4.3 (1) |
| C13 | −0.3292 (7) | 0.0402 (3) | 0.2059 (4) | 4.0 (1) |
| C14 | −0.4841 (7) | 0.1484 (3) | 0.3584 (4) | 4.3 (1) |
| C15 | −0.330 (1) | −0.0106 (3) | 0.1367 (5) | 7.2 (2) |
| C21 | 0.1937 (7) | 0.0405 (2) | 0.4723 (4) | 3.5 (1) |
| C22 | 0.2537 (8) | −0.0113 (3) | 0.4357 (4) | 4.4 (1) |
| C23 | 0.1886 (7) | −0.0117 (2) | 0.3411 (4) | 3.9 (1) |
| C24 | 0.2248 (8) | 0.0616 (3) | 0.5724 (4) | 4.7 (1) |
| C25 | 0.2080 (9) | −0.0582 (3) | 0.2679 (5) | 5.8 (2) |
| C31 | 0.1156 (6) | 0.2198 (2) | 0.2124 (3) | 2.8 (1) |
| C32 | 0.1377 (7) | 0.2004 (3) | 0.1250 (3) | 3.3 (1) |
| C33 | 0.0945 (6) | 0.1396 (3) | 0.1180 (3) | 3.1 (1) |
| C34 | 0.1498 (7) | 0.2813 (3) | 0.2556 (4) | 3.6 (1) |
| C35 | 0.0934 (8) | 0.0956 (3) | 0.0382 (4) | 4.5 (1) |
| C41 | −0.2012 (6) | 0.2358 (2) | 0.5057 (3) | 2.8 (1) |
| C42 | −0.3067 (7) | 0.2462 (3) | 0.6510 (4) | 4.3 (1) |
| C43 | −0.4608 (8) | 0.2110 (4) | 0.6447 (5) | 6.9 (2) |
| C44 | −0.3404 (8) | 0.3313 (3) | 0.5303 (4) | 4.9 (1) |
| C45 | −0.504 (1) | 0.3317 (4) | 0.4768 (7) | 9.8 (3) |
| B | −0.0147 (8) | 0.0608 (3) | 0.2303 (4) | 3.3 (1) |

[a] Anisotropically refined atoms are given in the form of the isotropic equivalent thermal parameter defined as $8\pi^2(U_{11} + U_{22} + U_{33})/3$.

**Table III.** Positional and Isotropic Thermal Parameters for $\{HB(Me_2pz)_3\}MoS(S_2CNEt_2)\cdot CH_2Cl_2$[a]

| atom | x | y | z | $B_{eq}$ (Å$^2$) |
|---|---|---|---|---|
| Mo | 0.44341 (6) | 0.00131 (4) | 0.09576 (2) | 2.656 (8) |
| Cl1 | 0.2983 (5) | 0.5225 (2) | 0.2166 (1) | 8.96 (8) |
| Cl2 | 0.3774 (7) | 0.3274 (2) | 0.2146 (1) | 11.3 (1) |
| S1 | 0.2368 (2) | 0.1004 (1) | 0.05366 (7) | 3.89 (4) |
| S2 | 0.5470 (3) | 0.0419 (1) | 0.01119 (7) | 3.99 (4) |
| S3 | 0.5730 (3) | 0.1011 (1) | 0.14143 (8) | 4.72 (4) |
| N11 | 0.3098 (7) | −0.1362 (3) | 0.0592 (2) | 2.7 (1) |
| N12 | 0.3086 (6) | −0.2145 (3) | 0.0899 (2) | 2.8 (1) |
| N21 | 0.2842 (7) | −0.0473 (3) | 0.1579 (2) | 2.7 (1) |
| N22 | 0.2924 (7) | −0.1379 (3) | 0.1757 (2) | 2.6 (1) |
| N31 | 0.6206 (6) | −0.1112 (4) | 0.1125 (2) | 2.9 (1) |
| N32 | 0.5715 (7) | −0.1900 (3) | 0.1386 (2) | 2.8 (1) |
| N41 | 0.337 (1) | 0.1570 (5) | −0.0393 (2) | 5.8 (2) |
| C11 | 0.2365 (9) | −0.1632 (5) | 0.0148 (3) | 3.3 (1) |
| C12 | 0.1901 (9) | −0.2553 (5) | 0.0179 (3) | 3.8 (2) |
| C13 | 0.2365 (9) | −0.2865 (5) | 0.0651 (3) | 3.3 (1) |
| C14 | 0.209 (1) | −0.1007 (6) | −0.0296 (3) | 4.5 (2) |
| C15 | 0.216 (1) | −0.3811 (5) | 0.0894 (3) | 4.9 (2) |
| C21 | 0.1822 (8) | −0.0011 (6) | 0.1899 (2) | 3.4 (1) |
| C22 | 0.125 (1) | −0.0616 (5) | 0.2276 (3) | 4.4 (2) |
| C23 | 0.198 (1) | −0.1474 (5) | 0.2174 (3) | 3.5 (1) |
| C24 | 0.139 (1) | 0.0988 (6) | 0.1841 (3) | 5.0 (2) |
| C25 | 0.169 (1) | −0.2381 (6) | 0.2444 (3) | 5.4 (2) |
| C31 | 0.7868 (8) | −0.1175 (5) | 0.1061 (3) | 3.4 (1) |
| C32 | 0.8433 (9) | −0.1994 (5) | 0.1286 (3) | 4.1 (2) |
| C33 | 0.7064 (9) | −0.2442 (5) | 0.1479 (2) | 3.3 (1) |
| C34 | 0.886 (1) | −0.0471 (6) | 0.0784 (4) | 5.4 (2) |
| C35 | 0.698 (1) | −0.3365 (5) | 0.1743 (3) | 5.0 (2) |
| C41 | 0.368 (1) | 0.1079 (5) | 0.0021 (3) | 3.9 (2) |
| C42 | 0.182 (2) | 0.2108 (6) | −0.0441 (3) | 9.2 (3) |
| C43 | 0.034 (2) | 0.159 (1) | −0.0646 (5) | 11.4 (4) |
| C44 | 0.467 (2) | 0.1670 (8) | −0.0824 (4) | 8.6 (3) |
| C45 | 0.420 (2) | 0.110 (1) | −0.1202 (6) | 13.0 (5) |
| C51 | 0.366 (2) | 0.4274 (7) | 0.2503 (4) | 7.4 (3) |
| B | 0.3844 (9) | −0.2129 (5) | 0.1436 (3) | 2.6 (1) |

[a] Anisotropically refined atoms are given in the form of the isotropic equivalent thermal parameter defined as $8\pi^2(U_{11} + U_{22} + U_{33})/3$.

Reactions which employed previously isolated samples of $MoO(S_2CNR_2)_2$ (eq 1) were equally successful. Due to the limited solubility of the reactants in toluene, the substitution reactions required ca. 18 h of reaction time. The formation of $Mo(S_2CNR_2)_4$[24] during the reactions was also noted (removed in washing procedure). With the exception of the soluble *n*-butyl derivative **1d** the complexes crystallized from the refluxing reaction mixture and were isolated by filtration in air. Chromatographic isolation of **1d** was required. Complexes **1a** and **1b** were first encountered as minor products of the aerobic workup of the reactions of tetraalkylthiuram disulfides and $(Et_4N)[\{HB(Me_2pz)_3\}Mo(CO)_3]$ in refluxing acetonitrile, which yield as major products the mononuclear $\eta^1$-dithiocarbamatomolybdenum(III) complexes $\{HB(Me_2pz)_3\}Mo(S_2CNR_2)(\eta^1\text{-}S_2CNR_2)$.[25] The general synthetic route outlined in eq 1 and 2 can be extended to other 1,1-dithioacid derivatives.[26]

The gold-yellow, diamagnetic, sulfido complexes **2a–2d** were produced in high yield by the reactions of the oxo analogues with boron sulfide, $B_2S_3$ (eq 3). Treatment of green solutions of **1a–1d**

$$\{HB(Me_2pz)_3\}MoO(S_2CNR_2) \xrightarrow[CH_2Cl_2]{B_2S_3} \{HB(Me_2pz)_3\}MoS(S_2CNR_2) \quad (3)$$

with solid $B_2S_3$ leads to the slow formation of brown suspensions containing **2a–2d** and several intensely colored byproducts. The reaction time (usually 24 h) may vary depending on the source and history of the boron sulfide. The sulfido complexes were recrystallized in pure form following the removal of excess $B_2S_3$ from the reaction mixture. Although relatively air-stable in the solid state, **2a–2d** are air-sensitive in solution. Thus, their synthesis, isolation, and solution study must be performed under anhydrous and anaerobic conditions. The byproducts of the reactions (total yield ca. 15%) included the binuclear Mo(V) complexes, *syn*-$\{HB(Me_2pz)_3\}MoS(\mu\text{-}S)_2MoS(S_2CNR_2)$.[27]

Boron sulfide has been employed in the sulfurization of ketones[28] and vanadyl[29] and *cis*-$MoO_2(ONR_2)_2$[10] complexes and in our hands has proved to be a versatile reagent for similar reactions with oxopolypyrazolylborate complexes. Interestingly, hexamethyldisilthiane, $(Me_3Si)_2S$, a reagent being increasingly exploited in transition metal centered oxo to sulfido conversion reactions,[30] fails to react with **1a–1d** at ambient temperature. The

(23) Chen, G. J.-J.; McDonald, J. W.; Newton, W. E. *Inorg. Chem.* **1976**, *15*, 2612–2615.

(24) Nieuwpoort, A.; Staggerda, J. J. *Recl. Trav. Chim. Pays-Bas.* **1976**, *95*, 250–254.

(25) (a) Young, C. G.; Roberts, S. A.; Enemark, J. H. *Inorg. Chim. Acta* **1986**, *114*, L7–L8. (b) Young, C. G.; Roberts, S. A.; Enemark, J. H. *Inorg. Chem.* **1986**, *25*, 3667–3671.

(26) For example, the reaction of $MoO\{S_2P(OR)_2\}_2$ complexes and K-$\{HB(Me_2pz)_3\}$ under similar conditions yields the blue complexes $\{HB(Me_2pz)_3\}MoO\{S_2P(OR)_2\}$ after chromatographic ($CH_2Cl_2$ on silica) purification.

(27) The binuclear complexes were chromatographically isolated ($CH_2Cl_2$/silica) from the final filtrate. An X-ray diffraction study of the ethyl derivative revealed a *syn*-$[Mo_2S_4]^{2+}$ core possessing both five- and six-coordinate centers formed by ligation of $S_2CNEt_2^-$ and $HB(Me_2pz)_3^-$, respectively. $\{HB(Me_2pz)_3\}MoS(\mu\text{-}S)_2MoS(S_2CNEt_2)\cdot{}^2/_3CH_2Cl_2$ crystallizes in the triclinic space group $P\bar{1}$ with $a$ = 12.103 (3) Å, $b$ = 16.107 (4) Å, $c$ = 26.404 (7) Å, $\alpha$ = 79.82 (2)°, $\beta$ = 82.00 (2)°, $\gamma$ = 85.51 (2)°, $V$ = 5009 Å$^3$, $Z$ = 6. The structure was solved by direct methods and difference Fourier methods. Refinement using 6218 reflections with $F_o^2 > 3^*\sigma(F_o^2)$ has progressed to $R_w$ = 0.080. The three inequivalent molecules possess slightly different conformations of the ethyl groups on the $S_2CNEt_2^-$ ligands. Full details of the structure will be published at a later date.

(28) (a) Dean, F. M.; Goodchild, J.; Hill, A. A. *J. Chem. Soc. A* **1969**, 2192–2195. (b) Jerumanis, S.; Lalanette, J. *Can. J. Chem.* **1964**, *42*, 1928–1935.

(29) (a) Callahan, K. P.; Durand, P. J. *Inorg. Chem.* **1980**, *19*, 3211–3217. (b) Sato, M.; Miller, K. M.; Enemark, J. H.; Strouse, C. E.; Callahan, K. P. *Inorg. Chem.* **1981**, *21*, 3571–3573.

Table IV. Selected Bond Distances (Å) and Angles (deg) in $\{HB(Me_2pz)_3\}MoE(S_2CNEt_2)$ (E = O, S)

| | E = O (1b) | E = S3 (2b) |
|---|---|---|
| Mo-E | 1.669 (3) | 2.129 (2) |
| Mo-S1 | 2.434 (1) | 2.436 (2) |
| Mo-S2 | 2.451 (1) | 2.431 (2) |
| Mo-N11 | 2.457 (4) | 2.435 (5) |
| Mo-N21 | 2.178 (4) | 2.176 (4) |
| Mo-N31 | 2.182 (3) | 2.186 (5) |
| S1-C41 | 1.724 (5) | 1.709 (7) |
| S2-C41 | 1.728 (4) | 1.726 (7) |
| C41-N41 | 1.319 (6) | 1.315 (8) |
| E-Mo-S1 | 100.5 (1) | 100.97 (8) |
| E-Mo-S2 | 99.7 (1) | 100.68 (7) |
| E-Mo-N11 | 168.9 (1) | 167.2 (1) |
| E-Mo-N21 | 94.1 (2) | 94.5 (1) |
| E-Mo-N31 | 94.0 (2) | 94.0 (1) |
| S1-Mo-S2 | 71.65 (4) | 71.29 (6) |
| S2-Mo-N31 | 98.8 (1) | 98.1 (1) |
| N21-Mo-N31 | 87.2 (1) | 89.5 (2) |
| S1-Mo-N21 | 99.0 (1) | 97.4 (1) |
| S1-Mo-N11 | 88.61 (9) | 89.9 (1) |
| S2-Mo-N11 | 89.1 (1) | 89.1 (1) |
| N11-Mo-N21 | 78.1 (1) | 77.3 (2) |
| N11-Mo-N31 | 77.9 (1) | 76.4 (2) |
| Mo-S1-C41 | 88.3 (2) | 88.8 (2) |
| Mo-S2-C41 | 87.7 (2) | 88.6 (2) |
| S1-C41-S2 | 111.8 (2) | 111.3 (4) |
| S1-C41-N41 | 123.8 (4) | 124.6 (6) |
| S2-C41-N41 | 124.4 (4) | 124.1 (6) |

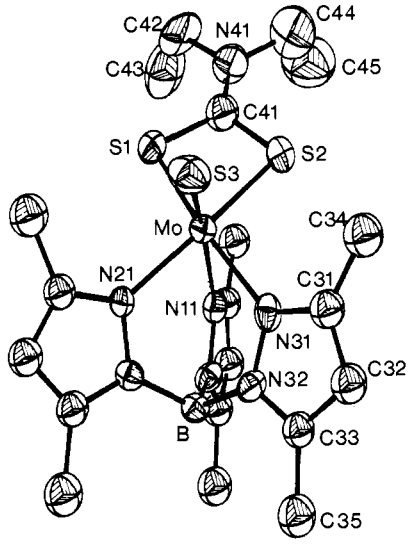


Figure 1. The molecular structure of $\{HB(Me_2pz)_3\}MoS(S_2CNEt_2)$ showing the atom labeling scheme. The numbering of atoms in the pyrazole rings containing N11 and N21 parallels that shown for the ring containing N31. Thermal ellipsoids are plotted at the 50% probability level and hydrogen atoms are not included. In the analogous structure of $\{HB(Me_2pz)_3\}MoO(S_2CNEt_2)$, the S3 atom is replaced the oxygen atom, O.

steric bulk of this reagent and the protection offered the Mo=O group by the 3-methyl substituents of $HB(Me_2pz)_3^-$ likely conspire to prevent reaction. This observation suggests that $(Me_3Si)_2S$ will have limited utility for oxo-to-sulfido conversion reactions involving metal complexes which possess sterically bulky coligands.

Table V. A Comparison of Oxo and Sulfido Ligation in Monomeric Complexes of Mo(IV)[a]

| complex | Mo=E distance (Å) | displacement of Mo from basal plane (Å) | ref |
|---|---|---|---|
| $(PPh_4)_3[MoO(CN)_5]$ | 1.705 (4) | 0.38 | 31 |
| $NaK_3[MoO_2(CN)_4]\cdot 6H_2O$ | 1.834 | 0.0 | 32 |
| $[Cr(en)_3][MoO(OH)(CN)_4]\cdot H_2O$ | 1.698 (7) | 0.21 | 33 |
| $[Pt(en)_2][MoO(OH_2)(CN)_4]\cdot 2H_2O$ | 1.668 (7) | 0.34 | 33 |
| $(PPh_4)_2[MoO(OH_2)(CN)_4]\cdot 4H_2O$ | 1.72 (2) | 0.35 | 31 |
| $(AsPh_4)_2[MoO(OH_2)(CN)_4]\cdot 4H_2O$ | 1.60 (2) | 0.38 | 31 |
| *trans*-$[MoOCl(CNMe)_4]I_3$ | 1.64 (4) | 0.33 | 34 |
| $CpMoO(CF_3C_2CF_3)(SC_6F_5)$ | 1.678 (5) | | 35 |
| $Na[MoO(CN)_3(phen)]\cdot 2phen$ | 1.659 (7) | 0.33 | 36 |
| $Na[MoO(CN)_3(phen)]\cdot 2phen\cdot MeOH\cdot H_2O$ | 1.669 (8) | 0.07 | 37 |
| MoO(TTP) | 1.656 (6) | 0.64 | 38 |
| MoO(phth) | 1.668 (8) | 0.69 | 39 |
| *cis*-$MoO(acac)_2(PMe_3)$ | 1.676 (5) | 0.29 | 40 |
| $[MoO(OH)(dppe)_2]BF_4$ | 1.833 (5) | 0.035 | 41 |
| *trans*-$[MoOCl(dppe)_2][ZnCl_3\cdot Me_2CO]$ | 1.69 | | 42 |
| $[MoOCl(dppe)_2][MoOCl_3(p\text{-}ClC_6H_4CON_2Ph)]$ | 1.71 (1) cation | 0.21 | 43 |
| | 1.62 (1) anion | 0.27 | |
| $MoOCl_2(PMe_2Ph)_3$ | 1.676 (7) | 0.211 | 44 |
| $MoOCl_2(PEt_2Ph)_3$ | 1.801 (9) | 0.123 | 45 |
| $[MoO(SH)([16]aneS_4)](SO_3CF_3)$ | 1.667 (3) | 0.07 | 46 |
| $MoO(SCH_2CH_2PPh_2)_2$ | 1.733 (9) | | 47 |
| $MoO(S_2CN\text{-}(i\text{-}Pr_2))_2$ | 1.664 (8) | 0.83 | 48 |
| $MoO(S_2CS\text{-}(i\text{-}Pr_2))_2$ | 1.66 (1) | 0.86 | 49 |
| $MoO(S_2C_2O_2)_2$ | 1.660 (8) | 0.71 | 50 |
| $MoO(S_2CPh)(S_3CPh)$ | 1.673 (2) | 0.81 | 51 |
| $(NEt_4)_2[MoO(S_4)_2]$ | 1.685 (7) | | 14 |
| $(PPh_4)_2[MoO(pdt)_2]$ | 1.667 (8) | | 52 |
| $\{HB(Me_2pz)_3\}MoO(S_2CNEt_2)$ | 1.669 (3) | 0.276 (1) | this work |
| $(NEt_4)_2[MoS(S_4)_2]$ | 2.128 | 0.725 | 14 |
| *trans*-$(PPh_4)_2[MoS(CS_4)_2]\cdot DMF$ | 2.126 (3) | 0.749 | 15 |
| $\{HB(Me_2pz)_3\}MoS(S_2CNEt_2)$ | 2.129 (2) | 0.2931 | this work |

[a] Abbreviations: en, ethane-1,2-diamine; cp, cyclopentadienide; phen, 1,10-phenanthroline; $H_2TTP$ tetratolylporphyrin; $H_2phth$, phthalocyanine; $H_2acac$, 2,4-pentandione; dppe, 1,2-bis(diphenylphosphino)ethane; $[16]aneS_4$, 1,5,9,13-tetrathiacyclohexadecane; pdt, 1,3-propandithiol; DMF, *N*,*N*-dimethylformamide.

**Description of Structures.** Positional and isotropic thermal parameters for the non-hydrogen atoms of **1b** and **2b**·$CH_2Cl_2$ are listed in Tables II and III, respectively. Selected bond lengths and angles for both molecules are presented in Table IV. The structure of **2b** is shown in Figure 1; the structure of **1b** is essentially identical, except for the presence of Mo=O instead of Mo=S. With the exception of the terminal chalcogenide (for **1b**, E = 0; for **2b**, E = S3), the atom labeling scheme (Figure 1) is identical for both **1a** and **2b**.

The unit cell of **1b** contains discrete monomeric molecules of $\{HB(Me_2pz)_3\}MoO(S_2CNEt_2)$ which exhibit distorted octahedral coordination about the molybdenum atom and possess approximate $C_s$ symmetry. The structural constraints of the $HB(Me_2pz)_3^-$ ligand restrict it to facial coordination sites. The Mo=O bond distance (1.669 (3) Å) is equal to the median value (1.67 Å) reported for 28 oxomolybdenum(IV) compounds (Table V).[14,31-52]

(30) For example: (a) Klemperer, W. G.; Schwartz, C. *Inorg. Chem.* **1985**, *24*, 4459–4461. (b) Money, J. K.; Huffman, J. C.; Christou, G. *Inorg. Chem.* **1985**, *24*, 3297–3302. (c) Do, Y.; Simhon, E. D.; Holm, R. H. *Inorg. Chem.* **1985**, *24*, 2827–2832. (d) Do, Y.; Simhon, E. D.; Holm, R. H. *Inorg. Chem.* **1985**, *24*, 1831–1838. (e) Sola, J.; Do, Y.; Berg, J. M.; Holm, R. H. *Inorg. Chem.* **1985**, *24*, 1706–1713. (f) Dorfman, J. R.; Girerd, J.-J.; Simhon, E. D.; Stack, T. D. P.; Holm, R. H. *Inorg. Chem.* **1984**, *23*, 4407–4412. (g) Minelli, M.; Enemark, J. H.; Wieghardt, K.; Hahn, M. *Inorg. Chem.* **1983**, *22*, 3952–3953.

(31) Wieghardt, K.; Backes-Dahmann, G.; Holzback, W.; Swiridoff, W. J.; Weiss, J. *Z. Anorg. Allg. Chem.* **1983**, *499*, 44–58.

(32) Day, V. W.; Hoard, J. L. *J. Am. Chem. Soc.* **1968**, *90*, 3374–3379.

(33) Robinson, P. R.; Schlemper, E. O.; Murmann, R. T. *Inorg. Chem.* **1975**, *14*, 2035–2041.

(34) Lam, C. T.; Lewis, D. L.; Lippard, S. J. *Inorg. Chem.* **1976**, *15*, 989–991.

(35) Howard, J. A. K.; Stansfield, R. F. D.; Woodward, P. *J. Chem. Soc., Dalton Trans.* **1976**, 246–250.

The well-documented structural trans influence of the terminal oxo ligand[14,38,39,47-52] which leads to relatively long bond distances to the trans ligand or to five-coordinate square pyramidal complexes is also reflected in the displacements of the Mo atom from the basal plane of ligands normal to the Mo=O group (Table V). For **1b** dissociation of the trans N11 atom is prevented by the tripodal coordination of the $HB(Me_2pz)_3^-$ ligand. However, the trans influence of the Mo=O group in **1b** lengthens the Mo–N11 bond (2.457 (4) Å) by ca. 0.28 Å compared to the Mo–N21 and Mo–N31 bonds which are cis to the Mo=O group, and the Mo atom is displaced 0.276 Å toward the oxygen atom from the plane defined by S1, S2, N21, and N31.

The structure of the related Mo(V) complex $\{HB(Me_2pz)_3\}$-$MoO(SPh)_2$[12a] provides an opportunity for direct comparison of oxomolybdenum(IV) and oxomolybdenum(V) centers in *fac*-$OS_2N_3$ coordination environments. The Mo(V) complex has a similar Mo=O bond distance (1.676 (4) Å); however, the trans Mo–N11 bond (2.357 (5) Å) is 0.10 Å shorter than for **1b**. The cis Mo–N21 and Mo–N31 distances do not differ significantly for the two complexes.

Bond lengths and angles within the $HB(Me_2pz)_3^-$ and $S_2CNEt_2^-$ ligands of **1b** are consistent with the values found for other complexes.[53,54] The C–N (1.319 (6) Å) and C–S (av 1.726 Å) bond distances of the dithiocarbamate ligand are intermediate between respective single and double bond distances (C–N = 1.47, C=N = 1.27, C–S = 1.81, C=S = 1.61 Å[55]) indicative of delocalized $\pi$-bonding in the $S_2CN$ portion of the ligand. As expected for a ligand with such thioureide character, the six atoms defining the rigid $S_2CNC_2$ skeleton of the ligand are coplanar (max displacement = 0.031 (5) Å, for N41). The dihedral angle between the $S_2C$ and $NC_2$ planes of the dithiocarbamate ligand is only 4.4°. The molybdenum atom is displaced, toward the oxygen atom, by 0.33 Å from the $S_2CNC_2$ plane.

The unit cell of **2b**·$CH_2Cl_2$ contains discrete monomeric molecules of $\{HB(Me_2pz)_3\}MoS(S_2CNEt_2)$ and dichloromethane. The general features of the **2b** molecule are essentially the same as those described above for **1b**. The six-coordinate molecule possesses a distorted octahedral coordination geometry and approximate $C_s$ symmetry. The Mo=S bond distance (2.129 (2) Å) is normal for a terminal sulfido group[14,15,56] (2.09–2.13 Å).

Table VI. Spectroscopic Data

| | infrared spectra[a] ($cm^{-1}$) | | | $^1$H NMR spectra[b] ($\delta$, $J$) | | | | | | | $^{95}$Mo NMR[d] electronic spectra[e,f] | | | |
|---|---|---|---|---|---|---|---|---|---|---|---|---|---|---|
| | | | | $S_2CNR_2^-$ ligand | | | | $HB(Me_2pz)_3^-$ ligand[c] | | | | | | |
| compd | $\nu$(BH) (m) | $\nu$(CN) (s) | $\nu$(Mo=E) (s) | C-1 | C-2 | C-3 | C-4 | *a*, *b* | *c*, *d* | *e* | *f* | $\delta$ | $W_{1/2}$ (Hz) | $\lambda$ | $\epsilon$ |
| **1a** | 2530 | 1535 | 956 | 3.60 | | | | 2.11, 2.22 | 2.45, 2.60 | 5.47 | 5.98 | 3000 | 2400 | 640, 446, 364 | 110, 310, 140 |
| **1b** | 2524 | 1510 | 954 | 4.03, ABX$_3$ $J_{AB}$ = 14.0, $J_{AX}$ = $J_{BX}$ = 7.5 | 1.43 t, $J$ = 7.5 | | | 2.16, 2.22 | 2.45, 2.61 | 5.47 | 5.98 | 3000 | 2040 | 638, 446, 362 | 110, 270, 165 |
| 1c | 2526 | 1505 | 954 | 3.91 s | 1.90 m | 1.04 t, $J$ = 7.5 | | 2.15, 2.21 | 2.44, 2.60 | 5.46 | 5.97 | 3000 | 1850 | 638, 448, 364 | 110, 290, 150 |
| **1d** | 2530 | 1506 | 955 | 3.95 m | 1.84 m | 1.44 m | 1.00 t, $J$ = 7.5 | 2.15, 2.21 | 2.44, 2.60 | 5.46[g] | 5.97 | 3000 | 3200 | 638, 446, 364 | 120, 305, 170 |
| **2a** | 2538 | 1535 | 512 | 3.73 s | | | | 1.94, 2.10 | 2.58, 2.94 | 5.23 | 6.13 | *h* | | 475 sh | 450 |
| **2b** | 2530 | 1505 | 512 | 4.22, ABX$_3$ $J_{AB}$ = 14.0, $J_{AX}$ = $J_{BX}$ = 7.5 | 1.51 t, $J$ = 7.5 | | | 2.00, 2.11 | 2.60, 2.94 | 5.25 | 6.14 | *h* | | 470 sh, 1060 | 540, 56 |
| 2c | 2526 | 1504 | 512 | 4.10 | 2.00 m | 1.08 t, $J$ = 7.5 | | 2.00, 2.10 | 2.60, 2.93 | 5.20 | 6.13 | *h* | | 470 sh | 520 |
| **2d** | 2530 | 1505 | 512 | 4.15 m | 1.93 m | 1.50 m | 1.03 t, $J$ = 7.5 | 2.00, 2.10 | 2.60, 2.94 | 5.24 | 6.13 | *h* | | 470 sh, | 510, 58 |

[a] As KBr disks: m = medium, s = strong intensity. [b] See text and Figure 2 for assignment labeling scheme; s = singlet, t = triplet, m = multiplet; $J$ values are in Hz, correct integrations were obtained. [c] All singlet resonances. [d] $\delta$ + 10. [e] $\lambda$ (nm). [f] $\epsilon$ ($M^{-1}$ $cm^{-1}$). [g] $CH_2Cl_2$ at 5.29. [h] Unobserved, $W_{1/2}$ > 4000 Hz.

(36) Basson, S. S.; Leipoldt, J. G.; Potgieter, I. M. *Inorg. Chim. Acta* **1984**, *87*, 71–78.
(37) Basson, S. S.; Leipoldt, J. G.; Potgieter, I. M. *Inorg. Chim. Acta* **1984**, *90*, 57–62.
(38) Diebold, T.; Chevrier, B.; Weiss, R. *Inorg. Chem.* **1979**, *18*, 1193–1200.
(39) Borschel, V.; Strahle, J. *Z. Naturforsch., B: Anorg. Chem., Org. Chem.* **1984**, *39B*, 1664–1667.
(40) Rodgers, R. D.; Carmona, E.; Galindo, A.; Atwood, J. L.; Canada, L. G. *J. Organomet. Chem.* **1984**, *277*, 403–415.
(41) Churchill, M. R.; Rotella, F. J. *Inorg. Chem.* **1978**, *17*, 668–673.
(42) Adams, V. C.; Gregory, U. A.; Kilbourne, B. T. *J. Chem. Soc., Chem. Commun.* **1970**, 1400–1401.
(43) Bishop, M. W.; Chatt, J.; Dilworth, J. R.; Hursthourse, M. B.; Motevalli, M. *J. Chem. Soc., Dalton Trans.* **1979**, 1603–1606.
(44) Manojlovic-Muir, L. *J. Chem. Soc. A.* **1971**, 2796–2800.
(45) Manojlovic-Muir, L.; Muir, K. W. *J. Chem. Soc., Dalton Trans.* **1972**, 686–690.
(46) DeSimone, R. E.; Glick, M. D. *Inorg. Chem.* **1978**, *17*, 3574–3577.
(47) Chatt, J.; Dilworth, J. R.; Schmutz, J. A.; Zubieta, J. A. *J. Chem. Soc., Dalton Trans.* **1979**, 1595–1599.
(48) Ricard, L.; Estrienne, J.; Karagiannidis, P.; Toledano, P.; Fischer, J.; Mitschler, A.; Weiss, R. *J. Coord. Chem.* **1974**, *3*, 277–285.
(49) Hyde, J.; Venkatasubramanian, K.; Zubieta, J. *Inorg. Chem.* **1978**, *17*, 414–426.
(50) Mennemann, K.; Mattes, R. *J. Chem. Res.* **1979**, 102.
(51) (a) Tatsumisago, M.; Matrsubayashi, G.; Tanaka, T.; Nishigaki, S.; Nakatsu, K. *J. Chem. Soc., Dalton Trans.* **1982**, 121–127. (b) Tatsumisago, M.; Matsubayashi, G.; Tanaka, T.; Nishigaki, S.; Nakatsu, K. *Chem. Lett.* **1979**, 889–890.
(52) Bishop, P. T.; Dilworth, J. R.; Hutchinson, J.; Zubieta, J. *J. Chem. Soc., Chem. Commun.* **1982**, 1052–1053.
(53) For $HB(Me_2pz)_3^-$, see: Lincoln, S.; Soong, S.-L.; Koch, S. A.; Sato, M.; Enemark, J. H. *Inorg. Chem.* **1985**, *24*, 1355–1359, and references therein.
(54) For $S_2CNEt_2^-$, see: Broomhead, J. A.; Sterns, M.; Young, C. G. *Inorg. Chem.* **1984**, *23*, 729–737, and references therein.
(55) Pauling, L. *The Nature of the Chemical Bond*, 3rd ed.; Cornell University Press: Ithaca, New York, 1960; p 260.
(56) Huneke, J. T.; Enemark, J. H. *Inorg. Chem.* **1978**, *17*, 3698–3699.

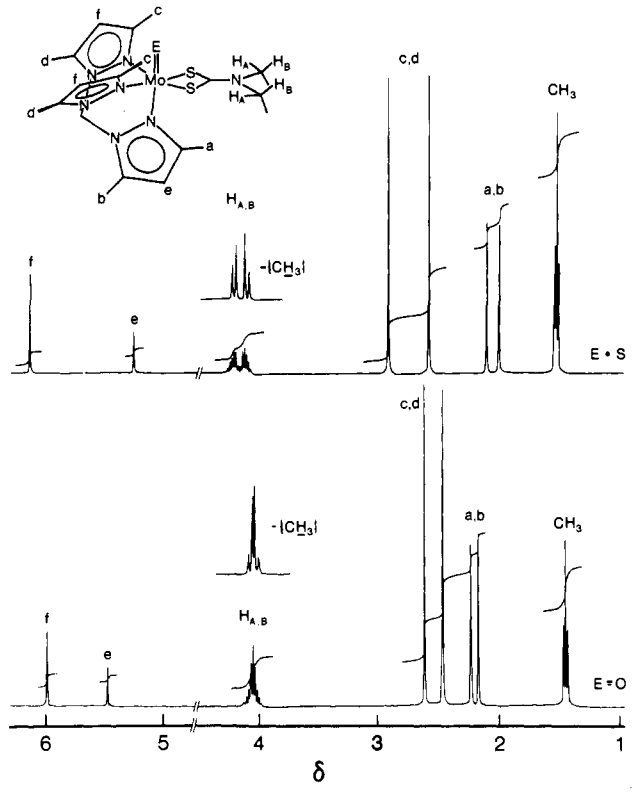


**Figure 2.** The 400-MHz $^1$H NMR spectra of $\{HB(Me_2pz)_3\}MoE(S_2CNEt_2)$ (E = O, S), in $CDCl_3/Me_4Si$. The structural formula shows the labeling scheme used in the assignment of these and other spectra (Table VI).

The Mo=S bond also exerts a strong structural trans influence, lengthening the Mo–N11 bond (2.435 (5) Å) by ca. 0.26 Å compared to the Mo–N21 and Mo–N31 bonds. The Mo atom is displaced toward S3 by 0.291 (1) Å from the plane defined by S1, S2, N21, and N31. The Mo–N21 and Mo–N31 distances and the bond lengths and angles within the $HB(Me_2pz)_3^-$ and $S_2CNEt_2^-$ ligands are consistent with those of **1b** and other complexes having these ligands.[53,54] The $S_2CNC_2$ skeleton is coplanar with a dihedral angle of 4.7° between the $S_2C$ and $NC_2$ planes. The Mo atom is displaced from the $S_2CNC_2$ plane toward the S3 atom by 0.12 Å. A comparison of this structure and those of other mononuclear sulfidomolybdenum(IV) complexes is given in Table V.

**Spectroscopy.** Spectroscopic data for the complexes are summarized in Table VI. The infrared spectra of **1a–1d** exhibit bands due to $HB(Me_2pz)_3^-$ ($\nu$(BH) ca. 2530 cm$^{-1}$), $S_2CNR_2^-$ ($\nu$(CN) ca. 1505 cm$^{-1}$), and terminal oxo ($\nu$(Mo=O) ca. 955 cm$^{-1}$) ligands. The absence of other bands in the 880–1000-cm$^{-1}$ region allows the unambiguous assignment of the $\nu$(Mo=O) vibration. Only one significant infrared spectral change accompanies the conversion of **1a–1d** to **2a–2d**; the strong $\nu$(Mo=O) band at 955 cm$^{-1}$ is replaced by a strong $\nu$(Mo=S) band at 512 cm$^{-1}$. Again, the absence of other ligand bands in the 500–600-cm$^{-1}$ region allows the unambiguous assignment of the $\nu$(Mo=S) vibration. The $[MoS(S_4)_2]^{2-}$ complex exhibits a band at 525 cm$^{-1}$ which has been similarly assigned.[14]

The 400-MHz $^1$H NMR spectra of complexes **1b** and **2b** are displayed in Figure 2, along with the labeling scheme used in the assignments given in Table VI. The spectra, particularly the resonance patterns produced by the $HB(Me_2pz)_3^-$ ligands, are consistent with molecular $C_s$ symmetry in solution. The mirror plane dictates the presence of six sets of equivalent protons in the $HB(Me_2pz)_3^-$ ligand; these are labeled a, b, c, d ($CH_3$ protons) and e and f (CH protons). Singlet resonances having the intensity ratio 3:3:6:6:1:2 may be readily assigned to these respective proton sets. In the assignments of the dithiocarbamate resonances, the protons involved are labeled according to the carbon atom to which they are attached. In complexes **1b** and **2b** the inequivalence of the methylene protons ($H_A$ and $H_B$) is readily discerned from the NMR spectra. In both spectra, an $ABX_3$ pattern characterizes these resonances. Decoupling of the adjacent $CH_3$ protons (Figure 2) causes the collapse of these resonances to the expected AB pattern ($J_{AB}$ = 14 Hz, $J_{AX} = J_{BX}$ = 7.5 Hz).

The $^{95}$Mo chemical shifts and line widths of **1a–1c** were reported recently as a part of a comprehensive $^{95}$Mo NMR study of mononuclear oxomolybdenum(IV) complexes.[22] The complexes exhibit very broad $^{95}$Mo NMR resonances at $\delta$ 3000 ± 10, toward the deshielded end of the chemical shift range established for mononuclear oxomolybdenum(IV) complexes ($\delta$ 3180 to 1035).[22] The broad resonances result from efficient quadrupolar relaxation of $^{95}$Mo, which is indicative of a large electric field gradient at the molybdenum nucleus in these molecules. Efforts to observe the resonances of **2a–2d** have been unsuccessful presumably due to their excessive line widths (>4000 Hz). This apparent increase in the line width of the resonances of **2a–2b** upon substitution of sulfur for oxygen contrasts with $MoE_2(ONR_2)_2$ complexes which have narrower $^{95}$Mo resonances when E = S. Previously, a deshielding effect of 500–700 ppm has been observed upon the replacement of a terminal oxo ligand by a terminal sulfido ligand in a variety of complexes, including molybdates and various group 11[57] derivatives thereof[58,59] and $MoE_2(ONR_2)_2$[30g] and $Cp_2Mo_2E_4$[60] complexes. On this basis the resonances of **2a–2d** would be expected to occur at ca. $\delta$ 3500–3700.

The electronic spectra of **1a–1d** exhibit absorption maxima at ca. 640, 446, and 364 nm, the last being a low intensity shoulder at the onset of intense UV absorptions. In contrast, the electronic spectra of **2a–2d** are devoid of absorption maxima in the visible region. The yellow color of the complexes is produced by the tailing of intense UV absorptions into the visible region. Weak shoulders are observed on the low-energy side of these intense absorptions, but their wavelength and extinction coefficients cannot be determined exactly. A weak near-IR band at ca. 1060 nm is probably the counterpart of the 640-nm band of **1a–1d**. Weak absorption bands at ca. 750 and 485 nm are sensitive indicators of impurities in samples of **2a–2d**.

The lowest energy band in each spectrum (640 nm, 15 600 cm$^{-1}$ when E=O and 1060 nm, 9430 cm$^{-1}$ when E=S) can be assigned to the $d_{x^2-y^2} \rightarrow d_{xz}$ and/or $d_{yz}$ transition.[61] Molecular orbital calculations[62] predict that the $d_{xz}$ and $d_{yz}$ orbitals are nearly degenerate in both types of complexes and are more destabilized with respect to the $d_{x^2-y^2}$ orbital in **1a–1d** than in **2a–2d**, consistent with the first electronic transition occurring at considerably higher energy in **1a–1d** than in **2a–2d**. The other d–d transitions in **1a–1d** occur at 446 nm (22 400 cm$^{-1}$, probably $d_{x^2-y^2} \rightarrow d_{xy}$) and 364 nm (27 500 cm$^{-1}$, probably $d_{x^2-y^2} \rightarrow d_{z^2}$). The middle transition ($d_{x^2-y^2} \rightarrow d_{xy}$) should be localized in the *xy* plane and therefore should be nearly independent of E atom type.[12b] A weak shoulder on the low-energy side of the charge-transfer band in **2a–2b** near

(57) The periodic group notation in parentheses is in accord with recent actions by IUPAC and ACS nomenclature committees. A and B notation is eliminated because of wide confusion. Groups IA and IIA become groups 1 and 2. The d-transition elements comprise groups 3 through 12, and the p-block elements comprise groups 13 through 18. (Note that the former Roman number designation is preserved in the last digit of the numbering: e.g., III → 3 and 13.)

(58) Gheller, S. F.; Hambley, T. W.; Rodgers, J. R.; Brownlee, R. T. C.; O'Connor, M. J.; Snow, M. R.; Wedd, A. G. *Inorg. Chem.* **1984**, *24*, 2519–2528, and references therein.

(59) Minelli, M.; Enemark, J. H.; Nicholson, J. R.; Garner, C. D. *Inorg. Chem.* **1984**, *23*, 4384–4386.

(60) Young, C. G.; Minelli, M.; Enemark, J. H.; Miessler, G.; Janietz, N.; Kauermann, H.; Wachter, J. *Polyhedron* **1986**, *5*, 407–413.

(61) Complexes **1** and **2** have effective $C_s$ symmetry as shown by NMR spectroscopy and X-ray crystallography. We have chosen the molecular coordinate system to conform to this symmetry with the *xz* plane as the mirror plane and the *z* axis along the Mo=E bond. In this coordinate system the $d_{x^2-y^2}$ orbital is the lowest energy d orbital, and its lobes are directed between the ligands in the *xy* plane normal to the Mo=E bond.

(62) Fenske–Hall molecular orbital calculations[65] on the model Mo(IV) complexes *fac*-$[(NH_3)_3MoO(S_2CNH_2)]^+$ and *fac*-$[(NH_3)_3MoS(S_2CNH_2)]^+$ show the same ordering of the metal d orbitals for both complexes. The HOMO is primarily $d_{x^2-y^2}$, the LUMO the nearly degenerate $d_{xz}$ and $d_{yz}$ orbitals. The calculated HOMO–LUMO gap is ca. 1.5 eV greater for the oxo compound than for the sulfido compounds.

**Table VII.** Electrochemical Data[a]

| compd | $E$ (V) | $E_p$ (mV) | $I_{pc}/I_{pa}$ |
|---|---|---|---|
| **1a** | 0.485 | | 1.0 |
| **1b** | 0.478 | 120 | 1.0 |
| **1c** | 0.474 | 115 | 1.0 |
| **1d** | 0.473 | 135 | 1.0 |
| **2a** | 0.282 | 125 | 0.69 |
| **2b** | 0.273 | 149 | 0.54 |
| **2c** | 0.274 | 210 | 0.67 |
| **2d** | 0.266 | | 0.80 |

[a] All measurements were made in 1 mM solutions of the compound in 0.05 M $Bu_4NBF_4/CH_2Cl_2$ at a glassy carbon electrode. Sweep rates were 50 mV/s.

440 nm may be the counterpart of this band. The charge-transfer transition in **2a–2d** from ligand orbitals to the $d_{xz}$ and/or $d_{yz}$ orbitals is shifted to sufficiently low energy to completely obscure any higher energy d–d transitions. The decrease in the energy of the ligand-to-metal charge-transfer transitions in **2a–2d** relative to **1a–1d** has two possible origins. First, the smaller destabilization of the $d_{xz}$ and $d_{yz}$ orbitals[62] in **2a–2d** noted above will also lower the energy of the charge-transfer transition in **2a–2d**. Second, there may be a change in the ligand orbitals participating in the lowest energy charge-transfer transition. For **1a–1d**, the transition will likely be from a dithiocarbamate ligand orbital, whereas in **2a–2d** the lowest energy charge transfer may involve the sulfur $p\pi$ orbitals of the Mo=S group.[62]

The band maxima of the lowest energy electronic transitions for **1a–1d** and for **2a–2d** are remarkably similar to the respective energies for the closely related molybdenum(V) compounds $\{HB(Me_2pz)_3\}MoECl_2$ (E=O, S).[12b] The lower energy observed when E = S compared to E = O for both the Mo(IV) and Mo(V) complexes further confirms the assignment of the lowest energy absorption to a transition which is essentially $d_{x^2-y^2} \rightarrow d_{xz}$ and/or $d_{yz}$. The interpretation of the electronic spectra is also consistent with the weaker $\pi$-donor ability of a sulfido vs. an oxo group.[12b]

The present results for $D^{2+}$ complexes (**2a–2d**) and previous results for $D^{3+}$ complexes[12b] suggest that sulfidomolybdenum(IV) and sulfidomolybdenum(V) complexes exhibit a characteristic electronic transition around 1000–1100 nm ($\epsilon \sim 50\ M^{-1}\ cm^{-1}$). If so, then near-IR spectroscopy is an important technique for identifying and characterizing $D^{2+,3+}$ complexes. However, the small absorption coefficient for the transition will make it difficult to use as a probe of $D^{2+,3+}$ centers in molybdenum enzymes.

**Electrochemistry.** Electrochemical data for **1** and **2** in dichloromethane are summarized in Table VII. As shown by cyclic voltammetry, the oxo complexes (**1a–1d**) undergo a quasi-reversible process at ca. 0.47 V (relative to SCE) ascribed to one-electron oxidation to the corresponding cationic oxomolybdenum(V) complexes. The potential of this process is nearly independent of the alkyl substituent on the dithiocarbamate ligand. The cationic oxomolybdenum(V) products of these oxidations are closely related to the stable, neutral oxomolybdenum(V) complexes of the type $\{HB(Me_2pz)_3\}MoOXY$ (X, Y = monoanions).[12] The latter complexes with X = Y = $SR^-$ undergo reversible one-electron reductions in the range −0.25 to −0.50 V.[12]

In freshly prepared dichloromethane solutions, the sulfido analogues (**2a–2d**) undergo an oxidation process at ca. 0.27 V (vs. SCE) that is not reversible ($I_c/I_a$ = 0.6–0.8). The potentials are independent of alkyl substituent on the dithiocarbamate ligand, and only one wave is observed from −0.2 to 1.2 V. However, smaller waves at 0.5 and 0.7 V appear after several scans on the same sample. When DMF is the solvent, all three anodic waves appear in the initial scan with roughly equivalent magnitudes, and all are largely irreversible. Figure 3 shows representative voltammograms for **1b** and for **2b** in dichloromethane and in DMF.

We infer that the initial oxidation product of **2** which gives rise to the first wave of the cyclic voltammogram at ca. 0.27 V undergoes further reactions to give electrochemically active intermediates responsible for the waves at 0.5 and 0.7 V. These reactions are much faster in DMF than in dichloromethane, and in DMF all three waves are observed in the first scan. The final

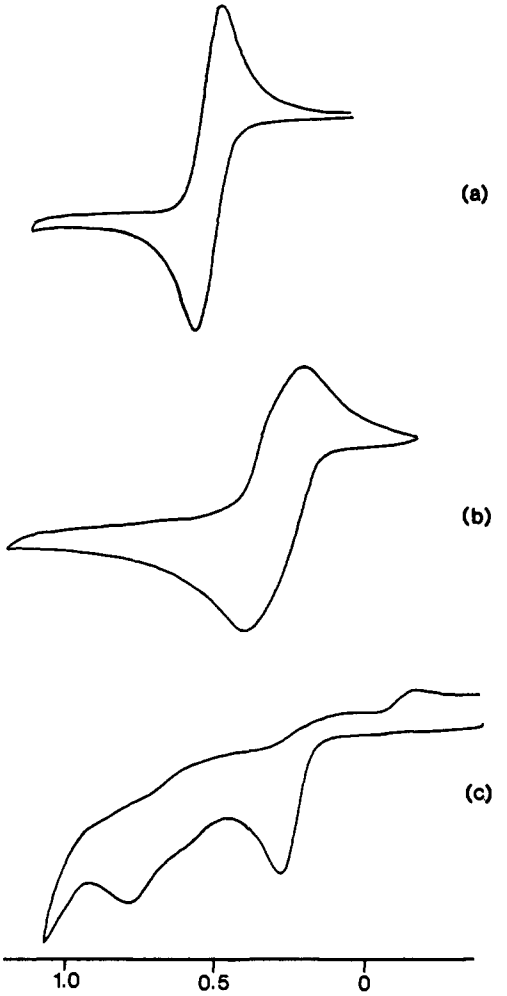


**Figure 3.** Cyclic voltammograms of 1 mM solutions of **1b** in $CH_2Cl_2$ (a), **2b** in $CH_2Cl_2$ (b), and **2b** in DMF (c). All were taken at a glassy carbon electrode with a scan rate of 50 mV/s.

oxidized products are not electrochemically reducible. In dichloromethane, the reaction of the initial oxidation product of **2** is slow on the CV time scale, and a few scans are possible before enough product is built up to allow the observation of the second and third waves. Scanning at slower rates or holding the potential at 0.4 V (just past the first wave) causes the second and third waves to grow in.

## Conclusion

The title complexes constitute the first series of analogous, indeed isostructural, six-coordinate oxo- and sulfidomolybdenum(IV) complexes. While six-coordinate oxomolybdenum(IV) complexes are quite common, there has been no previous report of a six-coordinate sulfidomolybdenum(IV) complex. The six-coordination of both the oxo and sulfido complexes can be ascribed to the preferred tripodal chelation of $HB(Me_2pz)_3^-$. Mononuclear sulfidomolybdenum(IV) complexes are rare in any case, and **2b** is only the third structurally characterized complex containing the $D^{2+}$ molybdenum center.[14,15]

This research further demonstrates the versatility of the $HB(Me_2pz)_3^-$ ligand for sterically moderating the chemistry of transition-metal complexes[63] and especially for stabilizing a variety of mononuclear molybdenum complexes which may be structural and spectroscopic models for the molybdenum centers of "oxo-type" molybdoenzymes. In addition to the examples of $C^{2+}$ and $D^{2+}$ complexes described here (compounds **1a–1d** and **2a–2d**, respectively), the $HB(Me_2pz)_3^-$ ligand has been used to prepare well-characterized examples of A ($\{HB(Me_2pz)_3\}MoO_2X$, X = monoanion[64]), $C^{3+}$ ($\{HB(Me_2pz)_3\}MoOXY$, X, Y = monoan-

(63) McCleverty, J. A. *Chem. Soc. Rev.* **1983**, *12*, 331–360.

ions,[12a] many of which incorporate biologically relevant sulfur-donor ligands), and $D^{3+}$ ($\{HB(Me_2pz)_3\}MoSCl_2$).[12b] These compounds and closely related derivatives provide important benchmark molecules for the development of multiple wavelength X-ray absorption spectroscopy and for the interpretation of X-ray absorption data from enzymes.[3]

The facile conversion of the six-coordinate oxomolybdenum(IV) complexes to their sulfido analogues is the first example of such a reaction for a pseudooctahedral mononuclear molybdenum center. Previous conversions have involved nonoctahedral stereochemistries or polynuclear metal centers.[8-10,29,30]

Finally, we note that the generally broad $^{95}Mo$ NMR signals for oxomolybdenum(IV) compounds and our inability to observe $^{95}Mo$ NMR spectra for the sulfidomolybdenum(IV) compounds offer little encouragement for the direct observation of such centers in enzymes by $^{95}Mo$ NMR.

(64) Young, C. G.; Cleland, W. E., Jr.; Enemark, J. H., manuscript in preparation.
(65) Hall, M. B.; Fenske, R. F. *Inorg. Chem.* **1972**, *11*, 768.

**Acknowledgment.** We thank Drs. B. R. James and I. S. Thorburn of the University of British Columbia for recording the 400-MHz $^1H$ NMR spectra, Dr. K. A. Christensen for assistance with the $^{95}Mo$ NMR spectroscopy, Dr. F. E. Mabbs and Dr. D. Collison for recording the near-IR spectra, and Dr. W. E. Cleland, Jr. for helpful discussions. Support of portions of this work by the U.S. Department of Agriculture (Grant 84-CRCR-1-1416) and the National Institutes of Health is gratefully acknowledged.

**Registry No. 1a**, 99113-26-5; **1b**, 99127-98-7; **1c**, 99127-99-8; **1d**, 107441-39-4; **2a**, 107441-40-7; **2b**, 107441-41-8; **2b**·$CH_2Cl_2$, 107441-44-1; **2c**, 107441-42-9; **2d**, 107441-43-0; *cis*-$MoO_2(S_2CNMe_2)_2$, 39248-36-7; *cis*-$MoO_2(S_2CNEt_2)_2$, 18078-69-8; *cis*-$MoO_2(S_2CNPr_2)_2$, 18078-70-1; *cis*-$MoO_2(S_2CNBu_2)_2$, 18078-71-2.

**Supplementary Material Available:** Tables of anisotropic thermal parameters, calculated hydrogen atom positions, and interatom distances and angles for $\{HB(Me_2pz)_3\}MoO(S_2CNEt_2)$ and $\{HB(Me_2pz)_3\}MoS(S_2CNEt_2)\cdot CH_2Cl_2$ (13 pages); structure factor tables for $\{HB(Me_2pz)_3\}MoO(S_2CNEt_2)$ and $\{HB(Me_2pz)_3\}MoS(S_2CNEt_2)\cdot CH_2Cl_2$ (31 pages). Ordering information is given on any current masthead page.

# Synthesis of *N,N'*-1,2-Vinylidene and 1,2-Phenylene Bridged Porphyrins. X-ray Crystal and Molecular Structure of an *N,N'*-(Diphenyl-1,2-vinylidene)-*meso*-tetraphenylporphyrin

**Henry J. Callot,*† Rémy Cromer,† Alain Louati,‡ Bernard Metz,§⊥ and Bernard Chevrier⊥**

*Contribution from the Laboratoire de Chimie Organique des Substances Naturelles (U.A. 31) and the Laboratoire d'Electrochimie et de Chimie Physique du Corps Solide (U.A. 405), Département de Chimie, Université Louis Pasteur, the Laboratoire de Chimie Minérale (U.A. 405), E.H.I.C.S., and the Laboratoire de Cristallographie Biologique, I.B.M.C. du C.N.R.S., Strasbourg, France.*
*Received October 31, 1986*

**Abstract:** The synthesis of *N,N'*-1,2-vinylidene and 1,2-phenylene bridged porphyrins, which are models of the inactivation products of cytochrome P-450 in the presence of 1-aminobenzotriazole (ABT) has been accomplished. They are prepared from *N*-aryl- or *N*-styrylporphyrins either by oxidation with amine cation radicals or electrochemically. Alternatively the direct reaction of a cobalt(III) porphyrin with ABT gave an *N,N'*-1,2-phenyleneporphyrin and an *N*-phenylporphyrin. The structure of an *N,N'*-(diphenyl-1,2-vinylidene)-*meso*-tetraphenylporphyrin, as its hydroperchlorate, was determined by X-ray crystallography. It showed (i) a considerable folding of the new seven-membered ring formed by the introduction of the 1,2-vinylidene group, (ii) that the protonated nitrogen atoms are the unsubstituted ones, and (iii) that the $\pi$-electron delocalization in the porphinato core is only moderately affected by the insertion of the two-carbon bridge.

The suicidal inactivation of cytochrome P-450 by 1-aminobenzotriazole (ABT) and related compounds[1,2] is of considerable interest since ABT, by itself of low toxicity, acts as an efficient synergist of insecticides[3] and herbicides[4] by inhibiting the cytochrome P-450 mediated detoxication pathways.

When, in 1981, Ortiz de Montellano and his collaborators[1] suggested structure **1** (4 isomers) as the modified porphyrinic component of deactivated cytochrome P-450, it was the first *N,N'*-phenylene bridged porphyrin, and even the first N–C–C–N bridged porphyrin, ever identified or synthesized. Only in 1984, when the full account of the isolation of the natural product was published,[2] appeared simultaneously in the literature[5] the preparation, by acid-catalyzed enamine formation, of an *N,N'*-vinylideneporphyrin **2**. This is in contrast with the series of one-carbon-bridged porphyrins which have been synthesized over the last 10 years.[6-8]

**Scheme I**

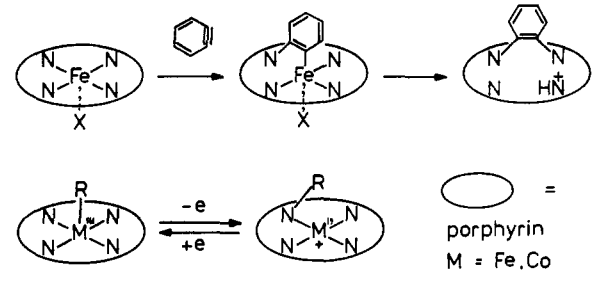


†U.A. 31, Département de Chimie.
‡U.A. 405, Département de Chimie.
§U.A. 405, E.H.I.C.S.
⊥I.B.M.C. du C.N.R.S.

(1) Ortiz de Montellano, P. R.; Mathews, J. M. *Biochem. J.* **1981**, *195*, 761-764.

0002-7863/87/1509-2946$01.50/0 